1 *Supplementary material for*

2 **Synergistic effects of Au and PdO$_x$ on the solar-assisted catalytic ozonation of**

3 **VOCs**

4

5

6 Junxian Gao[a], Zhizhang Shen[a], Yuming Dong[d], Zhenyu Wang[a], Jinze Lyu[a, c]*, Ji Li[a, c, e]*, Han-

7 Qing Yu[b]*

8 [a]School of Environment and Civil Engineering, Jiangnan University, Wuxi, Jiangsu, 214122, China

9 [b]Department of Environment Science and Engineering, University of Science and Technology of

10 China, Hefei, Anhui, 230026, China

11 [c]Jiangsu Key Laboratory of Anaerobic Biotechnology, Jiangnan University, Wuxi, Jiangsu, 214122,

12 China

13 [d]School of Chemical and Material Engineering, Jiangnan University, Wuxi, Jiangsu, 214122, China

14 [e]Jiangsu College of Water Treatment Technology and Material Collaborative Innovation Center,

15 Suzhou, Jiangsu, 215009, China

1 Catalytic experiments

2   The system was composed of a gas-distribution module, an ozone generator (COM-AD-01,

3 Anseros, Germany), a reactor, a xenon-lamp light source (Microsolar 300, Perfect Light, China), an

4 ultra-fine thermocouple, and a gas chromatography (GC) system (9790II, Fuli instrument, China).

5 High-purity air (composed of 79% N_2 and 21% O_2) was used as carrier gas. The total gas flow rate

6 was 510 mL/min. The concentrations of toluene, ozone, and H_2O were 140 mg/m³, 1000 mg/m³, and

7 12 580.9 mg/m³ (relative humidity at 25 °C was 50%). 0.1 g of the catalyst was uniformly coated onto

8 a 3.5 cm-diameter quartz plate, which was placed in the reactor. The gas hourly space velocity was

9 6000 h⁻¹. Full-spectrum light consists of IR, visible, and UV lights. The full-spectrum light intensity

10 was 450 mW/cm².

11   Toluene removal efficiency (X_{tol}), toluene mineralization efficiency (M), ozone removal efficiency

12 (X_{O3}), and CO_2 selectivity were calculated using Eq. (1)–Eq. (4), respectively.

13
$$X_{tol} = \frac{C_{tol,\,in} - C_{tol,out}}{C_{tol,\,in}} \times 100\% \tag{1}$$

14
$$M = \frac{C_{CO_2,out} - C_{CO_2,\,in}}{C_{tol,\,in} \times 3.35} \times 100\% \tag{2}$$

15
$$X_{O_3} = \frac{C_{O_3,\,in} - C_{O_3,out}}{C_{O_3,\,in}} \times 100\% \tag{3}$$

16   CO_2 selectivity
$$= \frac{C_{CO_2,out} - C_{CO_2,\,in}}{(C_{tol,\,in} - C_{tol,out}) \times 3.35} \times 100\% \tag{4}$$

17 where X_{tol} (%) and X_{O3} (%) represent the removal efficiency of toluene and ozone, respectively. M

18 represent the mineralization efficiency of toluene. $C_{tol,\,in}$ (mg/m³), $C_{CO2,\,in}$ (mg/m³), and $C_{O3,\,in}$ (mg/m³)

19 represent the concentrations of toluene, carbon dioxide, and ozone at the reactor inlet, respectively.

20 $C_{tol,\,out}$ (mg/m³), $C_{CO2,\,out}$ (mg/m³), and $C_{O3,\,out}$ (mg/m³) represent the concentrations of toluene, carbon

1 dioxide, and ozone at the reactor outlet, respectively.

2 The steady-state reaction rate (mg/(m³·min)) was calculated using Eq. (5).

3
$$r_{tol} = \frac{C_{tol,in} X_{tol} v}{V}$$
(5)

4 where v and V are the total flow rate (510 cm³/min) and reaction area volume (5.1 cm³), respectively.

5 The synergy factor of light and ozone was calculated using Eq. (6).

6
$$Synergy\ factor = \frac{r_{tol,PACO}}{r_{tol,O_3} + r_{tol,PCO}}$$
(6)

7 where $r_{tol,PACO}$, $r_{tol,O3}$, and $r_{tol,PCO}$ were the steady-state reaction rate of toluene in the presence of

8 ozone and light, in the presence of ozone only, and in the presence of light only, respectively.

9
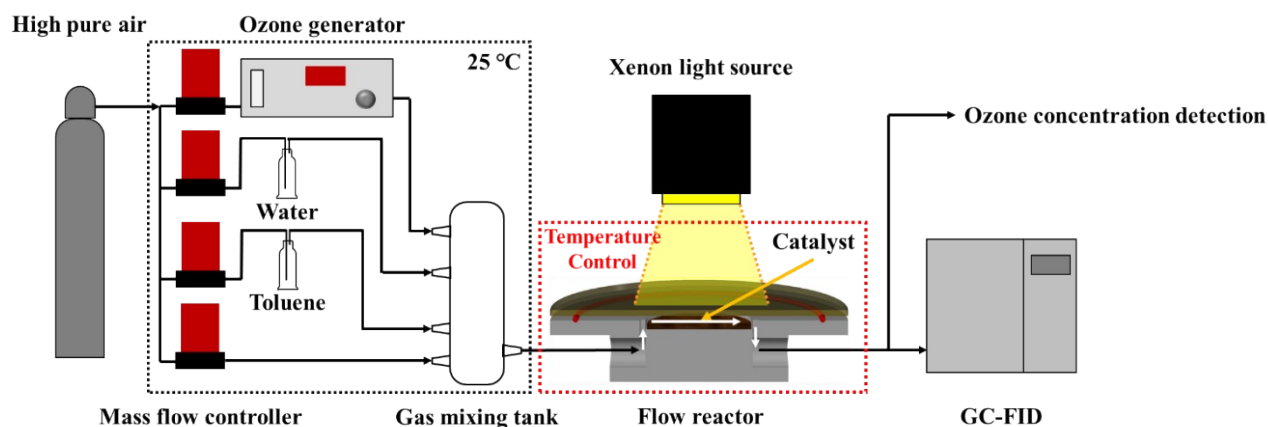
12 **Fig. S1.** Schematic of catalytic system

13

14 **Characterizations of catalysts**

15 The Ce content of the prepared samples was analyzed with an inductively coupled plasma optical

16 emission spectrometer (ICP-OES; Agilent 720ES, USA). The Au and Pd content of the prepared

17 samples was analyzed with an inductively coupled plasma mass spectrometer (ICP-MS; Agilent

1 ICPMS 7700, USA). X-ray diffraction (XRD) was measured by a X'Pert'3 Powder (Panalytical Co.,

2 Holland) with Cu Kα radiation. The surface element and electronic-structure of the prepared samples

3 were analyzed with an X-ray photoelectron spectroscopy (XPS) system (K-Alpha, Thermo Scientific

4 Inc., USA) with Al-Kα (hv=1486.6 eV) as X-ray source. The XPS curves were calibrated using the

5 adventitious carbon signal at 284.8 eV. UV-visible diffuse reflectance spectra were recorded by a UV-

6 visible spectrophotometer (UV-1800, SPC Co., China) with $BaSO_4$ as the reference sample. The

7 specific surface area of the samples was measured using a surface area analyzer (MicrotracBEL

8 Belsorp-Max Co., USA).

9

10 **Photothermal-conversion efficiency measurement**

11   0.1 g of catalyst was uniformly coated on the quartz plate, and the quartz plate was placed in the

12 reactor. The prepared sample on the quartz plate was heated by illumination. When the temperature of

13 the prepared sample was stable, the maximum temperature was recorded, and the light source was

14 turned off. The temperature of the prepared sample was measured by an ultrafine thermocouple. The

15 light power at the sample surface was measured by an optical power meter.

16   Photothermal conversion efficiency of absorption light and photothermal conversion efficiency

17 of incident light were calculated using Eq. (7) and Eq. (8), respectively.

18   Photothermal conversion efficiency of absorbed light (%): $\quad \eta_a = \dfrac{Q}{I}$ (7)

19   Photothermal conversion efficiency of incident light (%): $\quad \eta_i = \dfrac{Q}{I_{abs}}$ (8)

20 where Q (W), I (W), and I_{abs} (W) are the total heat of the prepared sample from absorbed light, incident

21 light power, and absorbed light power, respectively.

1   When the temperature of the prepared sample reached the maximum, the total generated heat was

2 equal to the total heat loss. Thus, Q was calculated using Eq. (9).

3     $Q = Q_{loss} = Q_{cond} + Q_{conv} + Q_{rad}$ (9)

4 where Q_{loss} (W), Q_{cond} (W), Q_{conv} (W), and Q_{rad} (W) are the total heat loss, heat conduction loss, heat

5 convection loss, and heat radiation loss, respectively. Considering that the contact area between the

6 quartz plate and the base in the test reactor was small, the conduction heat loss was negligible. The

7 heat convection loss was calculated using Eq. (10).

8     $Q_{conv} = hA(T_{max} - T_{surr})$ (10)

9 where h (W/[m^2·°C]), A (m^2), T_{max} (°C), and T_{surr} (°C) are the heat transfer coefficient, heat dissipation

10 area, maximum temperature of the prepared samples under illumination, and ambient temperature,

11 respectively. h was calculated using Eq. (11).

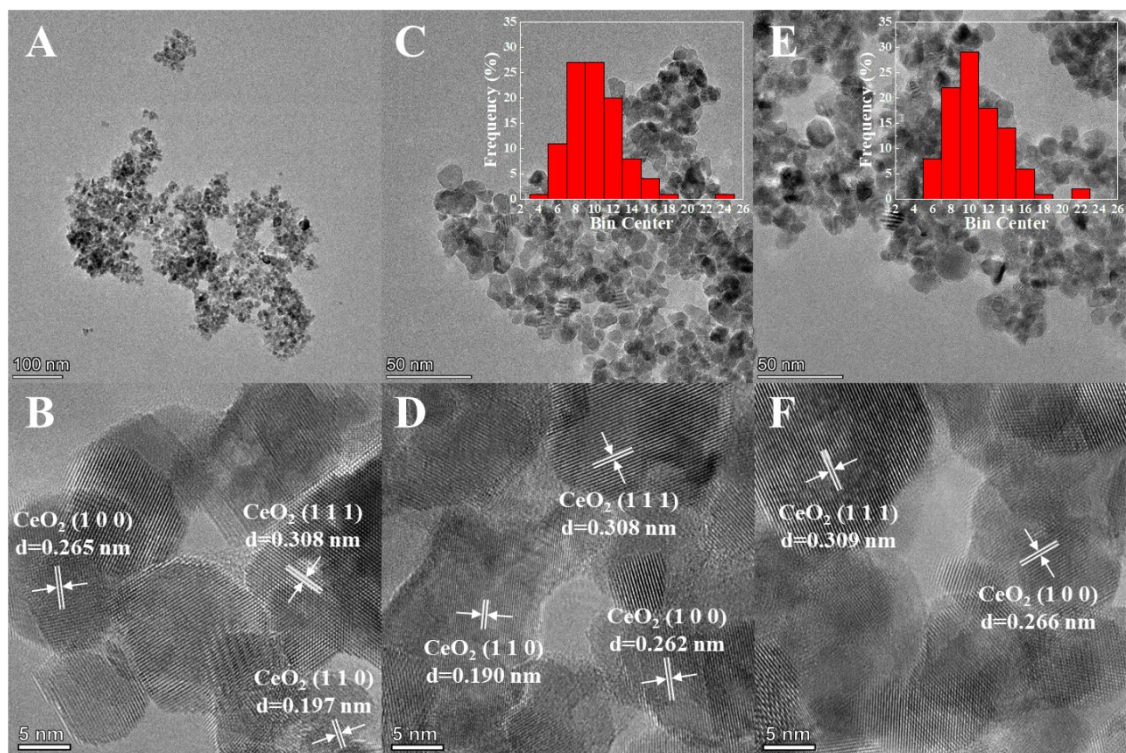12 $$h = 2.51C(\frac{T_{max} - T_{surr}}{L})^{0.25}$$ (11)

13 where C and L are the parameters determined on the basis of the shape of the quartz plate. The heat

14 radiation loss was calculated using Eq. (12).

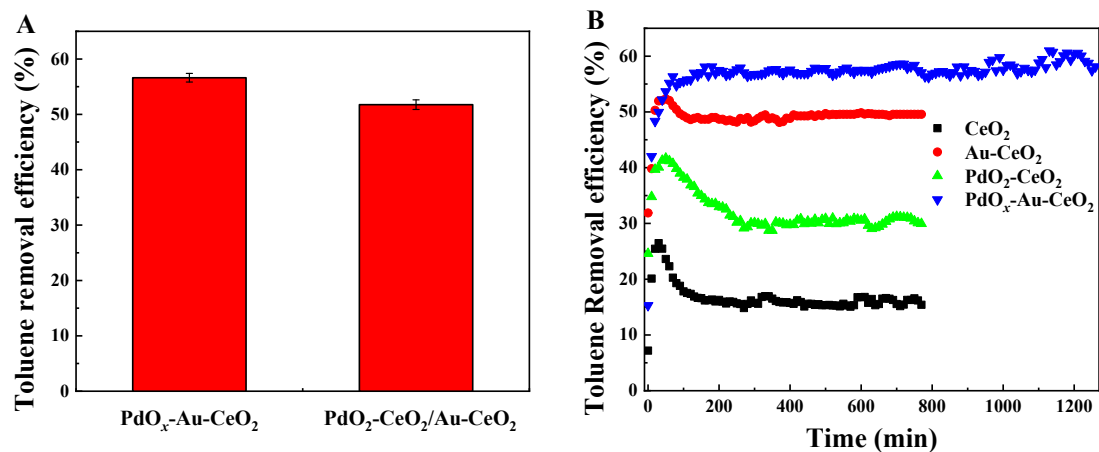15 $Q_{rad} = A\sigma\varepsilon(T_{max}{}^4 - T_{surr}{}^4)$ (12)

16 where σ is the Stefan–Boltzmann constant, 5.67×10^{-8} W/(m^2·K^4). ε is the radiation factor of the
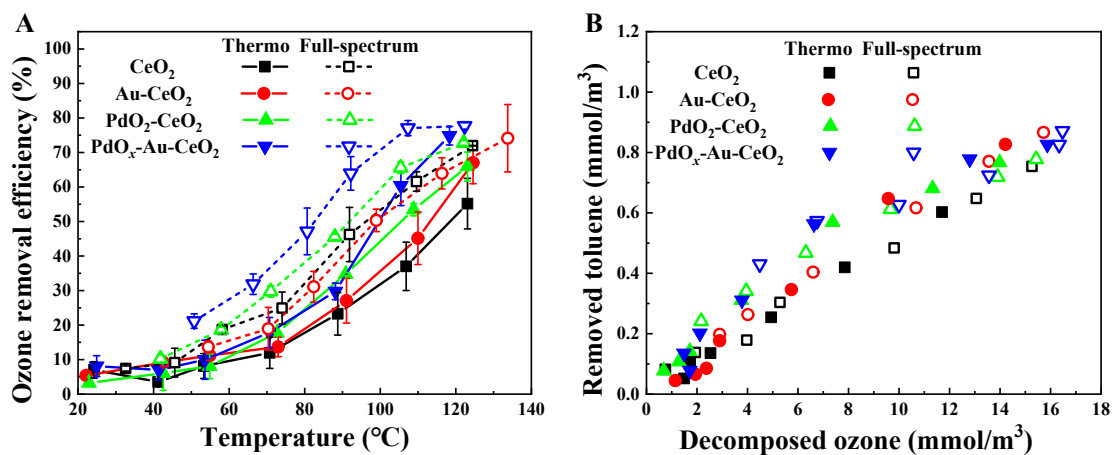
17 prepared samples.

18

19

Fig. S2. TEM images of CeO_2 (A), Au-CeO_2 (C), and PdO_2-CeO_2 (E). HRTEM images of CeO_2 (B), Au-CeO_2 (D), and PdO_2-CeO_2 (F).

Fig. S3. (A) Removal efficiencies of toluene for PdO_x-Au-CeO_2 and PdO_2-CeO_2/Au-CeO_2 in the presence of ozone and full-spectrum light; (B) Removal efficiencies of toluene for the prepared samples over time in the presence of ozone and full-spectrum light.

Fig. S4. Removal efficiency of ozone (A) and the correlation between decomposed ozone and removed toluene (B) with thermostatic control in darkness or under full-spectrum irradiation for the prepared samples.
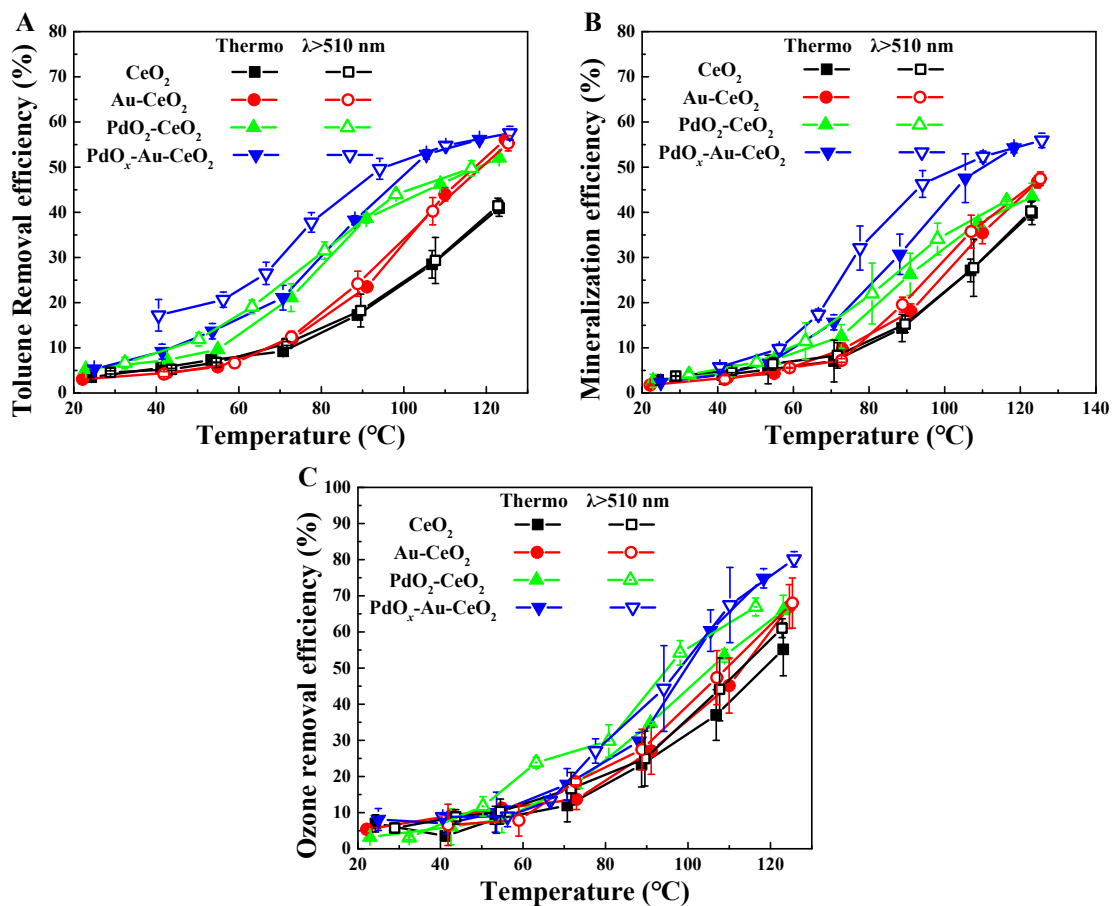
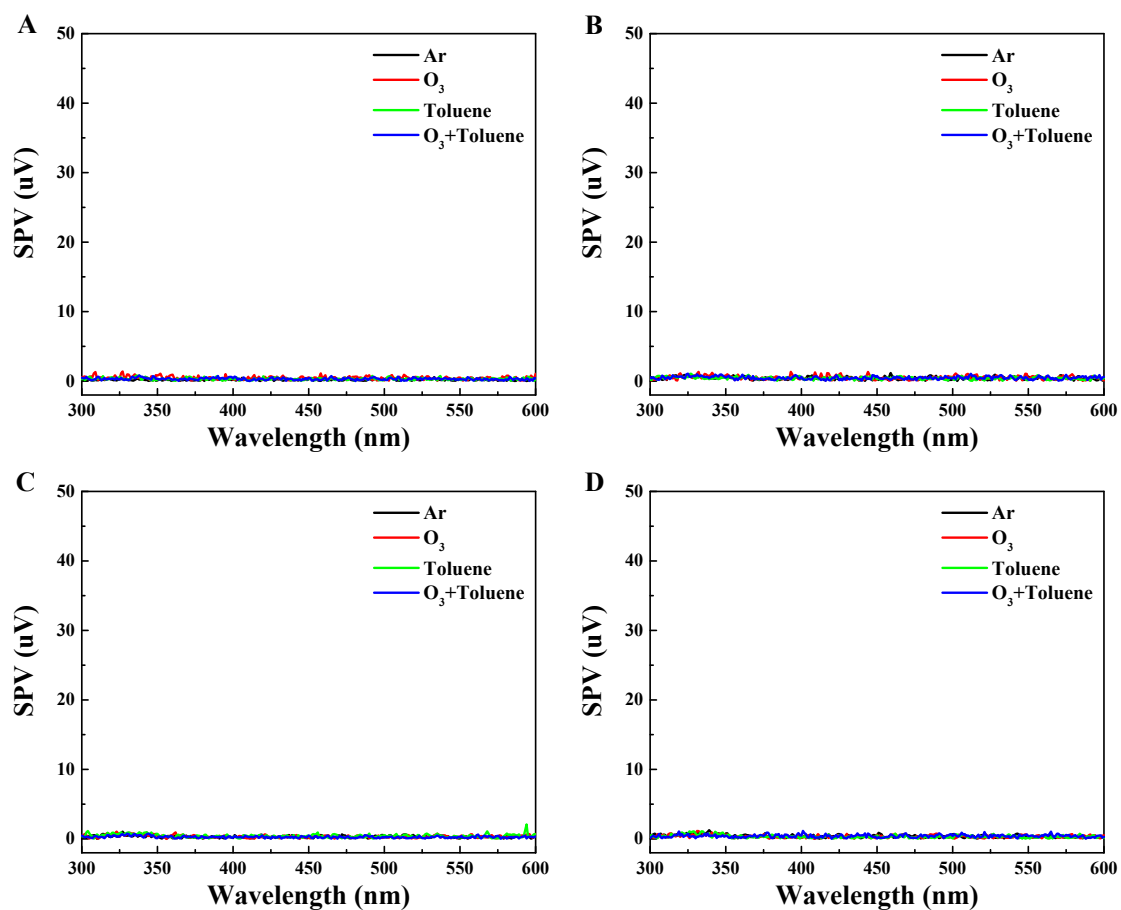**Fig. S5.** Removal efficiency of toluene (A), mineralization efficiency of toluene (B), and removal efficiency of ozone (C) with thermostatic control in darkness or under under light irradiation (> 510 nm) for the prepared samples.

Fig. S6. SPV spectra of CeO$_2$ (A), Au-CeO$_2$ (B), PdO$_2$-CeO$_2$ (C), and PdO$_x$-Au-CeO$_2$ (D) in Ar, O$_3$, toluene, and O$_3$+toluene atmospheres.

Table S1 Catalytic performance of catalysts and corresponding experimental conditions from other works

Catalyst	VOC	C_{VOC}^{a} (mg/m³)	C_{ozone}^{b} (mg/m³)	Light source	C_{Water}^{c} (mg/m³)	Hourly space velocity(/h)	r_{VOC}^{d} (mg/(m³·min))	Synergistic factor between light and ozone	References
TiO$_2$	Styrene	46.5	47.1	310−380 nm	12580.9	60	33.3	-	[14]
TiO$_2$	Ethylbenzene	346	16500	254 nm	10064.7	69.2	343.2	2.51	[15]
ZnO-GAC	Benzene	375	3572.1	365 nm	20479.1	21.6	107.8	1.21	[27]
TiO$_2$	Toluene	82.1	150	UVA	8200	150	205.3	-	[28]
TiO$_2$	n-decane	953.3	816	254 nm	10064.7	1800	5622.0	2.1	[29]
Cu$_2$O-CuO/TiFN	n-hexane	1346.6	342.9	254 nm+185 nm	11322.8	176.8	3015.7	-	[30]
TiO$_2$	Trichloroethylene	502.9	750.1	254 nm	20710	-	-	0.51	[31]
TiO$_2$	Trichloroethylene	502.9	750.1	365 nm	20710	-	-	0.91	[31]
TiO$_2$	Toluene	61.6	64.29	254 nm	8050	125	89.4	0.77	[19]
TiO$_2$	Toluene	61.6	64.29	365 nm	8050	125	44.7	2.4	[19]
TiO2/Zn-ZSM-5	acetaldehyde	528.4	280.7	254 nm	8200	-	-	0.83	[32]
TiO2/Cu-ZSM-5	acetaldehyde	528.4	280.7	254 nm	8200	-	-	0.97	[32]
TiO2/Mn-ZSM-5	acetaldehyde	528.4	280.7	254 nm	8200	-	-	1.08	[32]
TiO$_2$	1,2-dichlorobenzene	4086.6	235.7	365 nm	-	84.5	4431.6	-	[33]
TiO$_2$	Toluene	184.8	792.9	254 nm	10000	26.7	78.9	1	[34]
PdO$_x$-LaFeO$_3$	Toluene	135.7	1071.4	Xenon light, 447 mW/cm²	12580.9	6000	7178.5	3.82	Our previous work
PdO$_x$-Au-CeO$_2$	Toluene	140	1000	Xenon light, 447 mW/cm²	12580.9	6000	7864.3	8.94	This work

3 a. C_{VOC}: Initial concertration of VOC.

4 b. C_{ozone}: Initial concertration of ozone.

5 c. C_{water}: Initial concertration of water.

6 d. r_{VOC}: The removal amount of VOC per unit volume of catalyst per unit time.

7